2017

Design and verification of a hybrid nonlinear MRE vibration absorber for controllable broadband performance

Shuaishuai Sun
University of Wollongong, ssun@uow.edu.au

Tanju Yildirim
University of Wollongong, ty370@uowmail.edu.au

Jichu Wu
University of Wollongong

Jian Yang
University of Wollongong, yangj@uow.edu.au

Haiping Du
University of Wollongong, hdu@uow.edu.au

See next page for additional authors

Design and verification of a hybrid nonlinear MRE vibration absorber for controllable broadband performance

Abstract

In this work, a hybrid nonlinear magnetorheological elastomer (MRE) vibration absorber has been designed, theoretically investigated and experimentally verified. The proposed nonlinear MRE absorber has the dual advantages of a nonlinear force-displacement relationship and variable stiffness technology; the purpose for coupling these two technologies is to achieve a large broadband vibration absorber with controllable capability. To achieve a nonlinear stiffness in the device, two pairs of magnets move at a rotary angle against each other, and the theoretical nonlinear force-displacement relationship has been theoretically calculated. For the experimental investigation, the effects of base excitation, variable currents applied to the device (i.e. variable stiffness of the MRE) and semi-active control have been conducted to determine the enhanced broadband performance of the designed device. It was observed the device was able to change resonance frequency with the applied current; moreover, the hybrid nonlinear MRE absorber displayed a softening-type nonlinear response with clear discontinuous bifurcations observed. Furthermore, the performance of the device under a semi-active control algorithm displayed the optimal performance in attenuating the vibration from a primary system to the absorber over a large frequency bandwidth from 4 to 12 Hz. By coupling nonlinear stiffness attributes with variable stiffness MRE technology, the performance of a vibration absorber is substantially improved.

Disciplines

Engineering | Science and Technology Studies

Publication Details

Sun, S. S., Yildirim, T., Wu, J., Yang, J., Du, H., Zhang, S. W. & Li, W. H. (2017). Design and verification of a hybrid nonlinear MRE vibration absorber for controllable broadband performance. Smart Materials and Structures, 26 (9), 095039-1-095039-9.

Authors

Shuaishuai Sun, Tanju Yildirim, Jichu Wu, Jian Yang, Haiping Du, Shiwu Zhang, and Weihua Li

Design and verification of a hybrid nonlinear-MRE vibration absorber for controllable broadband performance

S.S. Sun[1], T. Yildirim[1], Jichu Wu[1], J. Yang[1], H. Du[2], S.W. Zhang*[3] and W.H. Li*[1]

[1]School of Mechanical, Materials and Mechatronic Engineering. University of Wollongong, Australia

[2]School of Electrical, Computer & Telecommunications Engineering, University of Wollongong, Australia

[3]Department of Precision Machinery and Precision Instrumentation, University of Science and Technology of China, China

*Corresponding author emails: weihuali@uow.edu.au; swzhang@ustc.edu.cn

Abstract

In this work, a hybrid nonlinear magnetorheological elastomer (MRE) vibration absorber has been designed, theoretically investigated and experimentally verified. The proposed nonlinear-MRE absorber has the dual advantages of a nonlinear force-displacement relationship and variable stiffness technology; the purpose for coupling these two technologies is to achieve a large broadband vibration absorber with controllable capability. To achieve a nonlinear stiffness in the device, two pairs of magnets move at a rotary angle against each other, and the theoretical nonlinear force-displacement relationship has been theoretically calculated. For the experimental investigation, the effects of base excitation, variable currents applied to the device (i.e. variable stiffness of the MRE) and semi-active control have been conducted to determine the enhanced broadband performance of the designed device. It was observed the device was able to change resonance frequency with the applied current; moreover, the hybrid nonlinear-MRE absorber displayed a softening-type nonlinear response with clear discontinuous bifurcations observed. Furthermore, the performance of the device under a semi-active control algorithm displayed the optimal performance in attenuating the vibration from a primary system to the absorber over a large frequency bandwidth from 4 Hz – 12 Hz. By coupling nonlinear stiffness attributes with variable stiffness MRE technology, the performance of a vibration absorber is substantially improved.

Keywords: *Magneto-rheological Elastomer absorber; Nonlinear broadband; Transmissibility; Semi-active control*

1. Introduction

The control of unwanted vibrations is of significant interest in many engineering applications; vibration control can improve performance, reduce damage to external components and increase the life span of many engineering systems, including, high speed trains, vehicles, tall buildings and bridges. To effectively suppress unwanted vibrations, the three most commonly investigated systems are damping systems, isolation systems and absorption systems [1-3]. Damping systems can attenuate the vibration by dissipating the ambient vibration energy into heat through viscoelastic materials, and isolator technology reduces the vibration transmission; however, a vibration absorber absorbs the energy from the primary system by matching its own natural frequency with the frequency of the excitation [4]. As the structure of the absorber is quite simple, it is robust and reliable and has been widely used in many areas after it was first proposed by Frahm [5].

Due to the working principle of an absorber, the performance of vibration suppression is significantly associated with the bandwidth of the device's own natural frequency. The traditional passive absorber only works efficiently in a very narrow bandwidth; in order to overcome issues associated with narrow bandwidth, variable stiffness magnetorheological elastomers (MREs) can be incorporated into an absorbers design [6, 7]. Magnetorheological elastomers, are a smart field-responsive material, that can increase their elastic modulus or stiffness monotonically under as an applied external magnetic field increases [8-10], and then immediately revert to their initial properties as the magnetic field is removed. This smart nature makes MRE ideal to develop semi-active absorbers. The incorporation of MRE into an absorber makes it possible to enable the natural frequency of the absorber controllable. In this way, an MRE absorber can deal with the variations in excitation frequency of different excitations. The first prototype of the MRE absorber was presented by Ginder *et al*. [11], and the experimental results showed that the bandwidth can cover a range from 500 Hz to 600 Hz. Deng *et al* [12, 13] later improved the design of Ginder *et al* by adding another wired coil along the magnetic path; when the current was

tuned from 0A to 1.5A, the resonant frequency changed from 55Hz to 81.25Hz, respectively. Subsequently, to improve the ability of addressing the large amplitude vibration of the MRE based absorber, Sun *et al* [4, 14] proposed a multilayered MRE absorber.

Although the MRE introduces adaptability in a vibration absorber, the effective operation bandwidth of the MRE absorber under constant current is still narrow; this limits the vibration suppression performance, as the vibration source in a practical environment always covers a large range of frequencies and is frequency variant. To deal with multi-frequency from the ambient environment, a nonlinear stiffness can be included in to expand the effective frequency bandwidth [15-17]. The original idea of a passive nonlinear absorber was investigated by Roberson [18]; this absorber consisted of a linear and hardening cubic spring; the conclusion of this investigation was that the nonlinear absorber can work in a much wider effective frequency bandwidth compared to its linear counterpart. This conclusion is further verified with experiments conducted by Arnold [19]. However, the existing nonlinear absorbers are not adaptive and cannot vary the device's own resonance frequency to match variations in the ambient excitation frequency.

Based on the literature, and the problems associated with tuneable devices and narrow bandwidth; this paper proposes an innovative hybrid nonlinear-MRE absorber, which combines the advantages of a nonlinear absorber and an MRE absorber to further increase the effective bandwidth of the device under a constant current and to realise its adaptability. As we shall see, by including both nonlinear broadband behaviour and variable stiffness magneto-rheological technology an enhanced broadband vibration absorber has been generated. The rest of this paper is organised as follows. The structure and analysis of the nonlinear MRE absorber is presented in Section 2. Section 3 illustrates the numerical simulation of the hybrid absorber and the experimental evaluation of the absorber is demonstrated in section 4. The vibration absorption performance of the absorber is evaluated in Section 5. Section 6 ends with concluding remarks.

2. The structure and analysis of the MRE absorber

In this section, a detailed description of the hybrid nonlinear-MRE absorber and associated components are discussed. The geometric relations for analysing the generated nonlinear force-displacement relationship and variable stiffness changes of the MRE are also discussed.

2.1 The structure of MRE absorbers

The newly designed MRE absorber is based on coupling a magnetically induced nonlinear stiffness with a multilayered MRE structure [20-22]. To combine the advantages of these two components, the new absorber has two essential parts; as shown in Fig.1, the main part of the absorber consists of a multilayered MRE structure with a permanent magnet in the middle, a solenoid, a steel cylinder, the top plate, bottom plate and the rotary arms mounted with two pairs of magnets. The multilayered MRE structure is composed of 10 layers of MRE films and 10 layers of thin steel circular plates. The thickness of the MRE and steel layers are both 1 mm. The MRE is fabricated with 70% carbonyl iron particles (C3518, Sigma-Aldrich Pty Ltd), 20% silicon sealant (Selleys Pty Ltd), and 10% silicon oil (Sigma-Aldrich Pty Ltd). The multilayered structure has been used as it can maintain the translational flexibility needed for large amplitude vibrations. The solenoid has 1000 turns and is used as the electro-magnet; a steel cover is mounted around the solenoid including the steel cylinder, top and bottom plates. The permanent magnet is used to provide an initial magnetic field to the MRE. The direction of the magnetic field generated by the solenoid can be the same with the initial magnetic field or opposite to the magnetic field when the current direction changes. As a result, the stiffness of the MRE structure can be stiffened or softened with the hybrid magnetic field.

The other important components are the rotary beams that are mounted on both sides of the absorber, as shown in Fig.1. As the stroke of the oscillator is limited, it cannot generate a nonlinearly induced stiffness in the MRE absorber, if the magnets are mounted on the oscillator directly. In order to solve this problem, two rotary beams working as mechanical amplifier are innovatively utilised in this device. One

end of the beam is hinged to the moving support on the translation track while the other end of the beam carries the magnets and is free to move. The beam is also hinged about point *O*, which is fixed to the bottom plate of the absorber (see Fig.1); moreover, the oscillator motion can induce the beam to rotate around point *O* and make the displacement of the stroke at the other end of the beam much larger. Two permanent magnets with opposite polarities are embedded into one end of the beam and the plastic support, respectively. The plastic support is fixed on the bottom plate, and the amplified relative motion between the two magnets is able to generate a nonlinear elastic restoring force within the MRE oscillator. The detailed dimensions of the MRE absorber are shown in Table 1. The m_a and m_b are the magnetic moment of the two magnets.

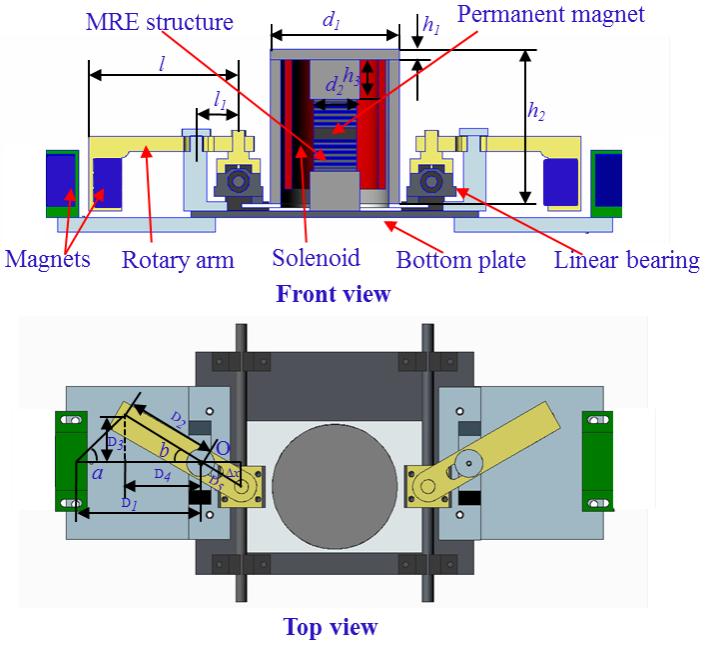

(a)

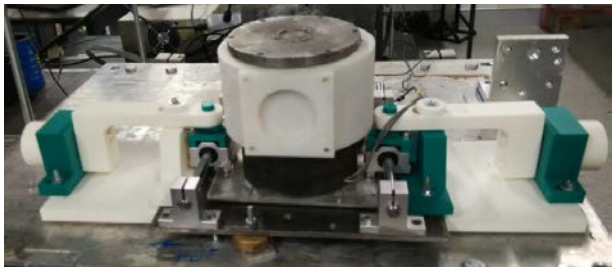

(b)

Figure 1: Structural design of the hybrid nonlinear-MRE absorber (a) schematic

representation; (b) photograph of the prototype

Table 1: Parameters of the hybrid nonlinear-MRE absorber

Parameters	Values		Parameters	Values
d_1	90mm		h_1	7mm
d_2	35mm		h_2	107mm
l	105mm		h_3	27mm
l_1	30mm		m_a	0.87
D_1	90mm		m_b	0.87

2.2 Analysis of multilayered MRE structure

The adaptability of the absorber is based on the adjustable stiffness of the MRE stack. In order to predict the different MRE stiffness under changing magnetism, and derive the frequency shift of the absorber, a theoretical analysis of the laminated MRE structure is conducted. The increased shear modulus of MRE layers under different magnetic field is given by [4]:

$$\Delta G = 36\emptyset\mu_0\mu_l\beta^2 \vec{H}_0{}^2 \left(\frac{d}{d_o}\right)^3 \zeta, \quad (1)$$

where $\beta=(\mu_p-\mu_l)/(\mu_p+2\mu_l)\approx 1$, $\mu_p\approx 1000$ and $\mu_l\approx 1$ are the relative permeability of the iron particles and silicon rubber, respectively; μ_0 is the vacuum permeability; d is the average particle radius, $\emptyset$ is the volume fraction, d_o is the particle distance before deflection, $\vec{H}_0$ is the intensity of the applied magnetic field, and $\zeta = \sum_{j=1}^{n} \frac{1}{j^3} \approx 1.202$.

The lateral stiffness of the i^{th} MRE sheet can be formulated as

$$k_{ti} = \frac{GA}{h} = \frac{(G_0+\Delta G)A}{h} = \frac{\left(G_0+36\emptyset\mu_0\mu_l\beta^2\vec{H}_0{}^2\left(\frac{d}{d_o}\right)^3\zeta\right)A}{h}, \quad (2)$$

where G is the overall shear modulus, G_0 is the initial shear modulus of the MRE, $\Delta G=G-G_0$ is the change of shear modulus under the magnetic field applied, h is the thickness of the MRE sheet and A is the effective area of an MRE sheet.

The lateral stiffness of the whole MRE structure which consists of 10 MRE sheets and 10 steel plates can be derived by the following equation

$$\frac{1}{k_{tw}} = \sum_{i=1}^{10} \frac{1}{k_{ti}} + \sum_{j=1}^{10} \frac{1}{k_{tj}}, \quad (3)$$

where k_{tw} is the overall lateral stiffness of the laminated MRE pillar, k_{tj} is the lateral stiffness of the steel sheet, as $k_{ti}<<k_{tj}$, the k_{tw} can be simplified as

$$k_{tw} = \frac{k_{ti}}{10} \ , \tag{4}$$

The natural frequency of the MRE structure can be calculated using

$$f_t = \frac{1}{2\pi}\sqrt{\frac{k_{tw}}{m}} \ , \tag{5}$$

where *m* is the mass of the oscillator. Substituting Eq. (2) and (4) into Eq. (5), the translational natural frequency can be obtained as

$$f_t = \frac{1}{2\pi}\sqrt{\frac{\left(G_0+36\emptyset\mu_0\mu_l\beta^2\vec{H}_0{}^2\left(\frac{d}{d_o}\right)^3\zeta\right)A}{10mh}} \ , \tag{6}$$

The intensity of the magnetic field $\vec{H}_0$ can be calculated by the method provided in the author's previous work using finite element analysis (FEA) [23]. On the basis of the above analysis, the relationship between the stiffness of the laminated MRE structure and current can be calculated as shown in Table 2.

Table 2: The relationship between the current and the stiffness of the laminated MRE structure

Currents (A)	Magnetic Flux Density (T)	Stiffness (N/m)
-2	0	1028
0	0.21	1727
2	0.26	2100
4	0.32	2649

2.3Nonlinear analysis

A nonlinear force is introduced by two pairs of permanent magnets. The nonlinear property induced by the magnetic system makes the MRE-based TMD have wider effective bandwidth under certain constant current. With this advantage, the nonlinear MRE absorber can well suppress the multi-frequency vibrations which widely exist in mechanical or structural systems while the ability of traditional semi-active TMDs to control these vibrations are limited because their frequency bandwidth under certain constant working conditions is still narrow.

The magnet with magnetic moment m_a is fixed on the plastic support on the bottom plate, and the other magnet with magnetic moment m_b is settled on the tip of

the rotary beam (see Fig 1.). Taking the left magnet pair as an example, the magnetic force between them keeps changing under a different rotary angle. The changing force provides the MRE absorber a nonlinear stiffness and influences the operation performance of the absorber. The magnetic force can be simplified as a dipole-to-dipole magnetic interaction force, and calculated as [24]

$$F = \frac{3\mu_0}{4\pi|r|^4}\left((\hat{r} \times m_a) \times m_b + (\hat{r} \times m_a) \times m_b - 2\hat{r}(m_b \cdot m_a) + 5\hat{r}((\hat{r} \times m_a) \cdot (\hat{r} \times m_b))\right), \quad (7)$$

where μ_0 is permeability of space ($4\pi e^{-7}\mathrm{Tm/A}$); $\hat{r}$ is the unit vector from m_a points to m_b and $|\boldsymbol{r}|$ is the distance between two magnet center. The magnet with magnetic moment m_a is fixed on the bottom plate so its position and orientation won't change while the magnet with magnetic moment m_b will change with the rotary arm. According to the geometry restriction shown in Fig.1 (a), the magnetic force line on the vector $\hat{k}$ can be formulated as

$$F_k = \frac{3\mu_0|m_a||m_b|}{4\pi|r|^4}(\sin(a) + \sin(a+b)\cos(b) + 2\sin(a+b)\cos(b) - 5\sin(a+b)\sin(a)\sin(a+b)), \quad (8)$$

As the input of the nonlinear magnetic force in this study is displacement Δx instead of angles a and b, the relationship between the angles and Δx needs to be formulated. According to the geometric relationship in Fig.1 (a), the geometric relationships can be formulated as

$$b = \mathrm{atan}\left(\frac{\Delta x}{l_1}\right), \quad (9)$$

$$D_5 = \sqrt{\Delta x^2 + l_1^2}, \quad (10)$$

$$D_2 = l - D_5, \quad (11)$$

$$D_3 = D_2\sin(b), \quad (12)$$

$$D_4 = D_2\cos(b) \quad (13)$$

$$a = \mathrm{atan}\left(\frac{D_3}{D_1 - D_4}\right) \quad (14)$$

The centre distance of the two magnets can be calculated by

$$|\mathrm{r}| = \sqrt{\mathrm{D}_3^2 + (\mathrm{D}_1 - \mathrm{D}_4)^2}\,, \tag{15}$$

As l, l_1, and D_1 are given in Table. 1, the relationship between displacement and the angles a and b can be obtained, and the nonlinear force-displacement relationship can be calculated. The nonlinear force is amplified by the lever amplifier; the mechanical gain factor is 2.33. There are two nonlinear force generating components in this structure and the nonlinear force working on the oscillator can be calculated by

$$F_n = 2.33 \times\ 2 \times \mathrm{F_k}\ , \tag{16}$$

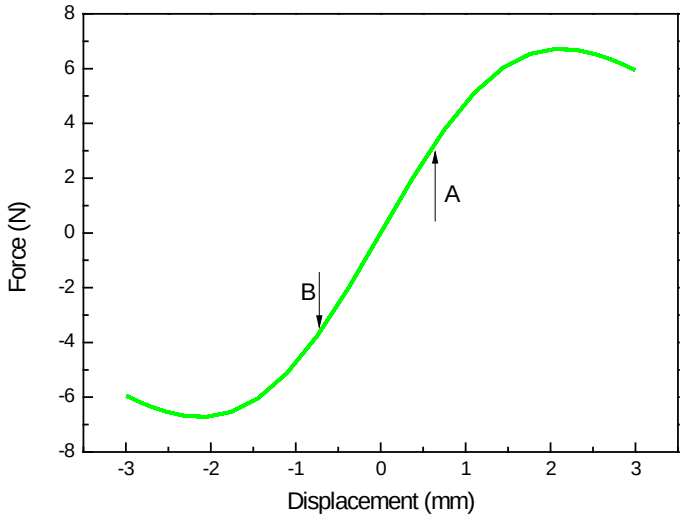

Figure 2: The relationship between the displacement and nonlinear elastic restoring force

According to Eqs. (8) – (16) and considering the real data of the MRE absorber in Table 1, the relationship of the magnetic force and the relative displacement can be simulated. The simulation result is presented in Fig. 2, for small displacements the force-displacement relationship tends to be linear denoted by the *AB* segment in Fig.2; however, for larger displacements (i.e. outside the *AB* segment), a nonlinear force displacement relationship is generated

3. Numerical simulation of the hybrid nonlinear-MRE absorber

A dynamic equation of motion can be used to predict and simulate the behaviour of the hybrid nonlinear-MRE absorber under an external excitation. The equation for translational response with nonlinear magnetic force can be expressed as

$$m\ddot{x} + c_{tw}(\dot{x} - \dot{x_0}) + k_{tw}(x - x_0) + F_n = 0 \ , \quad (17)$$

where x represents the translational response of the absorber under the excitation (i.e. the displacement field), x_0 is the input translational excitation; m=2kg, is the mass of the absorber, c_{tw} is the damping of the MRE. k_{tw} is the essential parameter for the MRE absorber as it controls the resonance frequency of the MRE absorber. The k_{tw} and F_n values calculated in the above section are used in this simulation. This dynamic equation including the nonlinear term was solved by numerical calculation technique using the Runge-Kutta method in MATLAB. The base excitation acceleration is 4.5m/s^2. The simulation results are presented in Fig. 3; the x axis is the frequency of excitation and y axis is the displacement of the oscillator relative to the bottom plate.

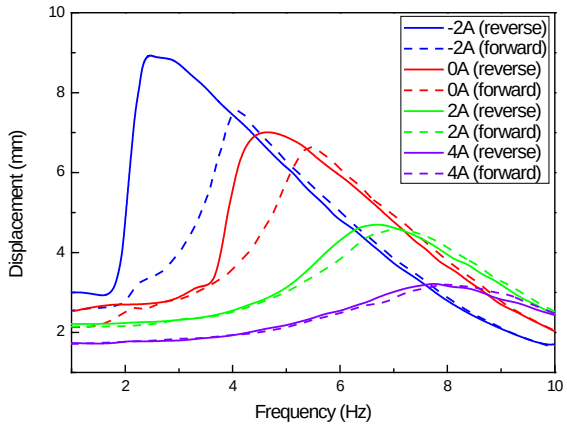

Figure 3: The frequency shift performance of the absorber under different currents

As shown in Fig. 3, the adaptability of the absorber and enhanced nonlinear bandwidth can be generated. The adaptability of the MRE absorber is controlled by the input current of the solenoid; with the current increasing, the natural frequency of the absorber increases due to the raising of the MRE stiffness. In this simulation, the source is a chirp signal with a sweeping range from 11Hz to 1Hz with the same excitation amplitude. Based on Fig. 3, it can be seen that with an increase of the MRE stiffness, the response displacement decreases, the nonlinear effect becomes less

obvious and the resonant frequency increases from 3.2Hz to 7.3Hz. Moreover, the dashed lines represent the frequency of the source signal for the forward sweeping direction from 1Hz to 11Hz. The forward sweep simulations have a similar trend of amplitude variation and frequency shift when compared to the reverse responses; however, when the stiffness is relatively small, the nonlinear response of the forward sweep is less obvious than the reverse sweep, the maximum resonant frequency is larger and the peak amplitude is smaller than the reverse sweep under the same stiffness. The difference between forward and reverse sweeps becomes small as the MRE stiffness increases.

4. Experimental test of the MRE absorber

The following section describes the interaction of system components and experimental procedure for evaluating the large broadband behaviour of the hybrid nonlinear-MRE absorber.

4.1 Experimental setup

The experiment in this section aims to test the dynamic properties of the MRE absorber designed in Section 2. Fig. 4 shows the prototype mounted on the experimental setup. In this experimental setup, the proposed absorber was fixed on the vibration platform excited by an electrodynamic shaker (VTS, .VC100-8). The excitation and the response of the absorber were measured by an accelerometer (CA-YD-106) and a laser sensor (MICRO-EPSILON Company), respectively. A DC power supply (THURLBY-THANDAR, INSTURMENTS LTD) was used to power the solenoid of the absorber. Between the hardware and software, a data acquisition (DAQ) board was used to transfer the information collected by the sensors to the computer; afterwards, all signal collection, recording and processing system were done using LabVIEW software.

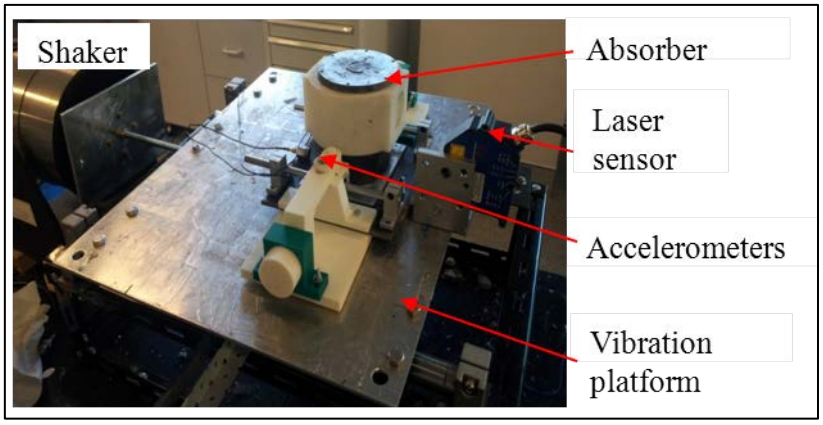

Figure 4: The experimental setup of the hybrid nonlinear-MRE absorber

When the shaker begins to work and excite the platform horizontally, the absorber attached on it will vibrate with it. With the vibration of the absorber, the relative motion between the two magnets will generate a nonlinear elastic restoring force to enlarge the effective frequency bandwidth of the absorber.

4.2 Testing result

Current variation

The frequency shift ability of the absorber under different currents were tested and analysed to illustrate its adaptability. The experimental results of the frequency shift properties with different solenoid currents under the same base excitation amplitude are shown in Fig. 5. The excitation from the shaker is a chirped signal, sweeping both forward and reverse directions from 3Hz to 10 Hz, with a 4.5m/s^2 base excitation acceleration, where the reversed response has been plotted by solid lines and the forward results are presented by the dashed lines.

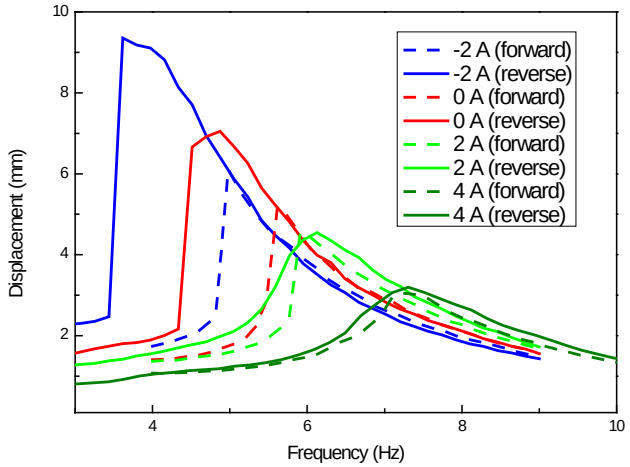

Figure 5: The experimental results of frequency shift performance

The relative displacement response under various current levels from -2A to 4A with step of 2A was collected. The results are shown in the form of the displacement of the oscillator. It can be seen that the resonance frequency increased from 3.6Hz to 7.3Hz as the current was increased from -2A to 4A, respectively. These results demonstrate the adaptability under the nonlinear working mode. When the current is small, the stiffness of the MRE is small and the nonlinear bandwidth was more prevalent. The frequency-response curve rises abruptly before it reached the highest point and a discontinuous bifurcation was observed experimentally, these points occurred as jump and down points for the forward and reverse sweeping direction, respectively. This property of a nonlinear stiffness effectively enlarges the working frequency bandwidth of the absorber. It was also observed in Fig. 5 that the nonlinear bandwidth is less obvious for the forward sweep compared to the reverse sweep under the same current.

Comparing the results of the experiment and the simulation in Section 3.3, it can be concluded that the theoretical analysis of the translational response can describe the frequency shift property very well. In summary, the adaptability of the hybrid nonlinear-MRE absorber can be realised by modifying current.

Effect of base excitation amplitude on the nonlinear working mode

As analysed in section 2, the magnetic nonlinear elastic restoring force is sensitive to the relative displacement of the two magnets, and the hybrid absorber will be sensitive to different base excitation amplitudes. In order to test its performance subject to different base excitations, different excitation levels are used to test the absorber performance. The sweeping excitation frequency range was from 4Hz to 9 Hz and the current in the solenoid was 0A during the test; as shown in Fig.6, the two base acceleration amplitudes used were 4.5m/s^2 and 3.5m/s^2.

It was observed that the frequency-response of the hybrid absorber displayed a linear response when the amplitude was 3.5m/s^2; the resonant frequency was 7.5Hz and the displacement under a forward sweep matches well with the reverse sweep. When the base excitation was increased to 4.5m/s^2, a nonlinear frequency-response curve was evident, jump up and down points corresponding to bifurcations in the frequency-space parameter were observed and the bandwidth of the hybrid nonlinear-MRE absorber was substantially enlarged. The response of the reverse sweep covers a far wider effective frequency bandwidth compared to the forward sweep. The different response between the two excitation levels is due to the nonlinear force model proposed in Section 3.1. Connecting with the analysis of Fig.2, it is known that the relationship between magnetic force and displacement tends to be linear when the excitation is small (in the *AB* segment), however, when the excitation is fierce enough the magnetic force begins to exhibit nonlinear behaviour. When the excitation amplitude is 3.5 m/s^2, the magnetic force is linear and when the excitation amplitude is 4.5m/s^2, the magnetic force exceeds the *AB* range and displays nonlinear behaviour. As a result, the absorber under 3.5 m/s^2 excitation is representative of a linear absorber and the absorber under 4.5 m/s^2 excitation is representative of a nonlinear absorber. Comparing their performance in Fig. 6, it can be concluded that the effective frequency bandwidth of the proposed nonlinear MRE absorber is much wider than that of a linear absorber.

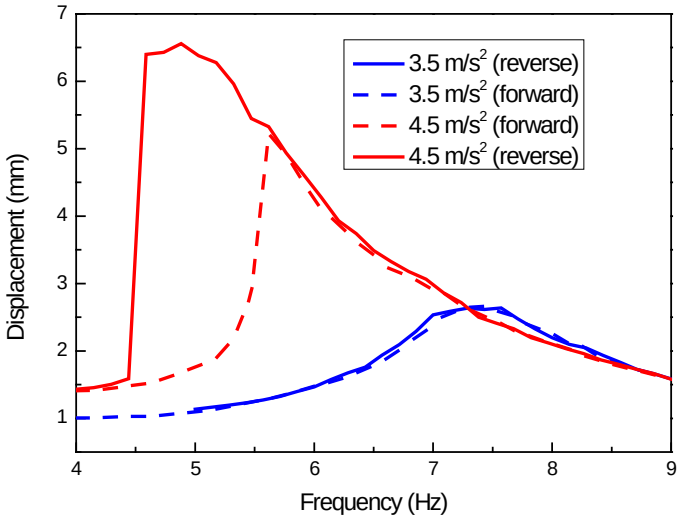

Figure 6: Response of the hybrid nonlinear-MRE absorber under different base acceleration amplitudes

5 Vibration reduction evaluations

The following section describes the experimental evaluation of vibration attenuation for a primary system using the nonlinear-MRE absorber; moreover, experiments for the semi-active control of the device have been conducted to further investigate the enhanced performance of the device.

5.1 Experimental system setup

To evaluate the vibration absorption performance of the hybrid absorber, a vibration absorption evaluation system which includes a primary system is built. The mass of the primary is 6.5kg. This system is similar to the system described in Fig. 4, in which the same hardware and software were used, except the primary system representing the object whose vibration needs to be controlled. The primary system was fixed on the vibration platform driven by the shaker and the absorber was fixed on the top plate of the primary system. Two accelerometers were set up to record the motion of the controlled primary system and the excitation as shown in Fig. 7.

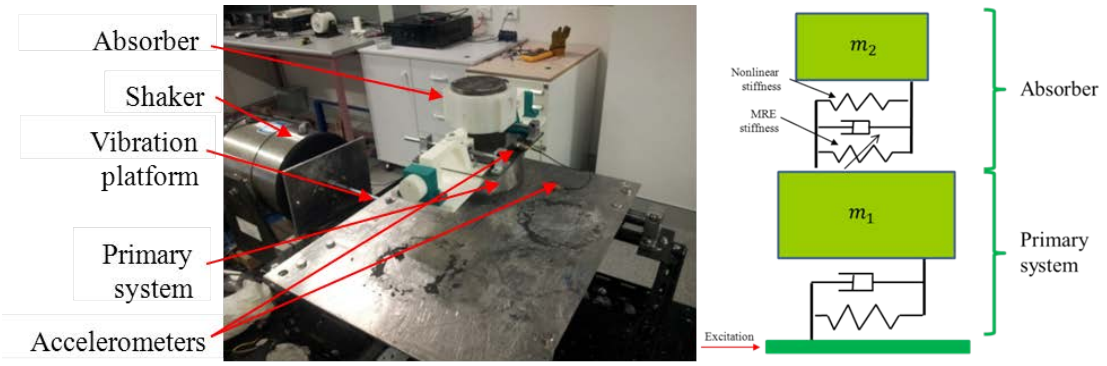

Figure 7: Photograph of the experimental setup for the vibration attenuation system

The signals collected by two accelerometers were recorded by the computer and the transmissibility of them was used to show the vibration absorption performance of the proposed absorber. The transmissibility is defined as the ratio between the primary system acceleration and the excitation acceleration. As a result, low transmissibility means better vibration attenuation performance and the appearance of a lowest value of the transmissibility, means the attenuation effectiveness is the best at that point. At that point the absorber reached its resonant frequency and absorbed most of the vibration energy so that the vibration of the primary system was reduced. The lowest point on the transmissibility curve is the best vibration absorption point of the absorber.

5.2 Testing results

Various base excitation amplitudes

As the absorber is sensitive to excitation amplitude, its performance under different base acceleration levels is evaluated first. The vibration attenuation effectiveness under different excitation amplitudes with the same current is shown in Fig. 8. The excitations are in the form of a chirped signal sweeping in the reverse direction from 12Hz to 3Hz, with the excitation amplitudes of 4.5m/s^2, 4 m/s^2 and 3.5 m/s^2, respectively; no current was applied to the excite MRE. The transmissibility under the three base excitation amplitudes have sunken shapes, this means that the absorber showed good vibration attenuation performance. It is also easy to find that three of curves have a sharp increase after the resonant frequency of the absorber, this represented that the oscillator continued resonating and absorb the vibration energy

over a larger bandwidth. Comparing the three curves in Fig.8, the important conclusion is drawn that with increased base excitation amplitude, the effective absorption bandwidth is wider due to the coupled magnetically induced nonlinear stiffness.

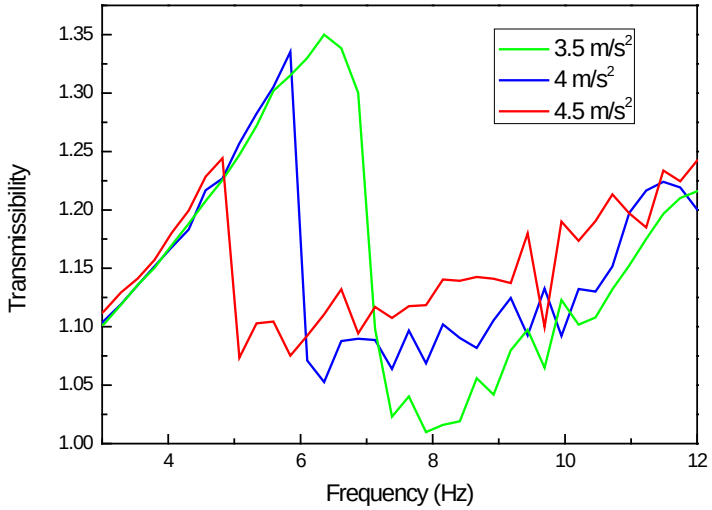

Figure 8: The vibration attenuation performance under different excitation amplitudes

Different current and semi-active control

Having analysed the impact of different base excitation amplitudes on the performance of vibration suppression; in this part, the response under variable currents are tested and analysed. The frequency range of the excitation was from 3Hz to 12Hz, sweeping in the reverse direction and the excitation amplitude is maintained at 4.5m/s^2 during the entirety of the experiment. The current is changed from 0A to 4A with a step of 1A. As shown in Fig. 9, the lowest point of transmissibility occurred at the resonant frequency and afterwards shifted towards the right with respect to the x-axis. The reason for the frequency shift is due to the increased current which adversely increased the magnetic field passing through the hybrid nonlinear-MRE absorber; this caused an increased stiffness of the MRE layers and the natural frequency of the device increased accordingly. Moreover, all the curves show clear nonlinear responses. The lowest points for each curve occurred when the absorber presents the best vibration attenuation performance at a specific current. So if all these lowest points can be connected and the absorber can be controlled by a semi-active

control technique, that tracks this optimal curve automatically, the absorber effectiveness will be improved dramatically. The red line in Fig.9 shows the semi-active control of the nonlinear-MRE absorber. In a semi-active system, sensors and controller are used to collect and process the acceleration signals, respectively and then give the suitable current for specific situation by STFT control algorithm. The control system is the same with the author's prior work [4]. Then the absorber will adjust its stiffness to track the excitation frequency variation. Comparing the transmissibility curve of the system with absorber and the system without the absorber (green line), it can be concluded that the all kinds of absorbers suppressed the vibration effectively. It also can be seen that the controlled absorber outperforms the other passive MRE absorber by comparing their vibration absorption performances.

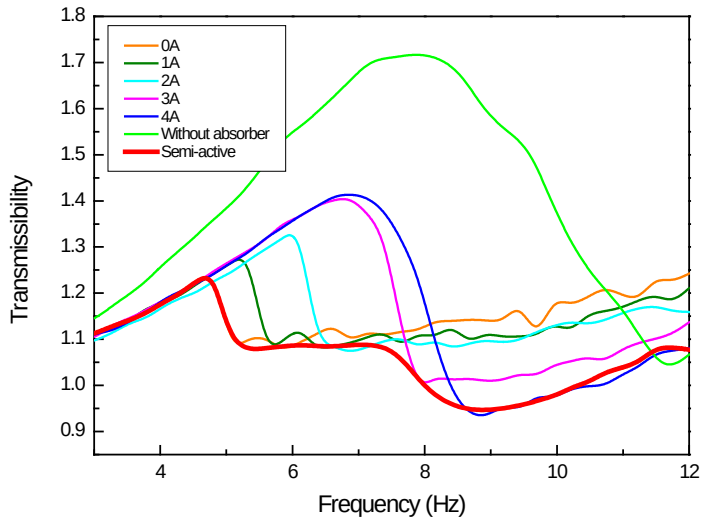

Figure 9: The vibration attenuation performance of different systems

6. Conclusion

In this work, magnetorheological elastomers (MRE) and a magnetically induced nonlinear force-displacement relationship have been coupled for the design and fabrication of an innovative hybrid nonlinear-MRE absorber. To verify the advantages of the proposed absorber, theoretical and experimental investigations have been performed for the translational motion of the system. It was observed the hybrid absorber displayed a softening-type nonlinear behaviour with the frequency-response

curves leaning towards the left. With an increased magnetic field applied to the MRE layer, the natural frequency of the device increased, which verified its adaptability; the experimental result also demonstrated the nonlinear-MRE absorber has boarder effective bandwidth than its linear counterpart under constant current. To further validate the enhanced performance of the device, evaluation of the nonlinear-MRE absorber on vibration absorption were conducted. It was shown that the nonlinear-MRE absorber outperforms other absorbers on vibration attenuation. In summary, using the added advantages of a nonlinearly induced magnetic stiffness, variable stiffness magneto-rheological technology and semi-active control technology, an adaptive broadband vibration absorber has been designed and validated.

Acknowledgements

This research is supported by ARC Grants (DP150102636, LP150100040).

References

[1] H. D. Chae and S. B. Choi, "A new vibration isolation bed stage with magnetorheological dampers for ambulance vehicles," *Smart Materials and Structures,* vol. 24, Art No. 017001, 2015.

[2] Z. Xu, X. Gong, G. Liao, and X. Chen, "An active-damping-compensated magnetorheological elastomer adaptive tuned vibration absorber," *Journal of Intelligent Material Systems and Structures,* vol. 21, pp. 1039-1047, 2010.

[3] C. Yang, J. Fu, M. Yu, X. Zheng, and B. Ju, "A new magnetorheological elastomer isolator in shear–compression mixed mode," *Journal of Intelligent Material Systems and Structures,* vol. 26, pp. 1290-1300, 2015.

[4] S. Sun, H. Deng, J. Yang, W. Li, H. Du, G. Alici*, et al.*, "An adaptive tuned vibration absorber based on multilayered MR elastomers," *Smart Materials and Structures,* vol. 24, Art No. 045045, 2015.

[5] F. H, "Device for Damping Vibration of Bodies," US patent, *989958*, ed, 1911.

[6] C. Peng and X. L. Gong, "Active-Adaptive Vibration Absorbers and its Vibration Attenuation Performance," *Applied Mechanics and Materials,* vol. 312, pp. 262-267, 2013.

[7] Z. Yang, C. Qin, Z. Rao, N. Ta, and X. Gong, "Design and analyses of axial semi-active dynamic vibration absorbers based on magnetorheological elastomers," *Journal of Intelligent Material Systems and Structures,* vol. 25, pp. 2199-2207, 2014.

[8] M. Behrooz, X. Wang, and F. Gordaninejad, "Performance of a new magnetorheological elastomer isolation system," *Smart Materials and Structures,* vol. 23, Art No. 045014, 2014.

[9] I. Agirre-Olabide, J. Berasategui, M. J. Elejabarrieta, and M. M. Bou-Ali, "Characterization of the linear viscoelastic region of magnetorheological elastomers," *Journal of Intelligent Material Systems and Structures,* vol. 25, pp. 2074-2081, 2014.

[10] L. Chen, X. Gong, and W. Li, "Effect of carbon black on the mechanical performances of magnetorheological elastomers," *Polymer Testing,* vol. 27, pp. 340-345, 2008.

[11] J. M. Ginder, W. F. Schlotter, and M. E. Nichols, "Magnetorheological elastomers in tunable vibration absorbers," in *SPIE's 8th Annual International Symposium on Smart Structures and Materials*, 2001, pp. 103-110.

[12] H. Deng, X. Gong, and L. Wang, "Development of an adaptive tuned vibration absorber with magnetorheological elastomer," *Smart Materials and Structures,* vol. 15, Art No. N111, 2006.

[13] H. Deng and X. Gong, "Application of magnetorheological elastomer to vibration absorber," *Communications in Nonlinear Science and Numerical Simulation,* vol. 13, pp. 1938-1947, 2008.

[14] S. Sun, J. Yang, W. Li, H. Deng, H. Du, and G. Alici, "Development of an MRE adaptive tuned vibration absorber with self-sensing capability," *Smart Materials and Structures,* vol. 24, Art No. 095012, 2015.

[15] L. Tang, Y. Yang, and C. K. Soh, "Improving functionality of vibration energy harvesters using magnets," *Journal of Intelligent Material Systems and Structures,* vol. 23, pp. 1433-1449, 2012.

[16] L. Zhao, L. Tang, and Y. Yang, "Enhanced piezoelectric galloping energy harvesting using 2 degree-of-freedom cut-out cantilever with magnetic interaction," *Japanese Journal of Applied Physics,* vol. 53, Art No. 060302, 2014.

[17] N. A. Alexander and F. Schilder, "Exploring the performance of a nonlinear tuned mass damper," *Journal of sound and vibration,* vol. 319, pp. 445-462, 2009.

[18] R. E. Roberson, "Synthesis of a nonlinear dynamic vibration absorber," *Journal of the Franklin Institute,* vol. 254, pp. 205-220, 1952.

[19] F. Arnold, "Steady-state behavior of systems provided with nonlinear dynamic vibration absorbers," *Journal of Applied Mechanics,* vol. 22, pp. 487-492, 1955.

[20] Y. Zhou, W. H. Li, and M. N. S. Hadi, "Performance comparison between an MRF damper and an MRE isolator incorporated with a building structure," *Applied Mechanics and Materials,* vol. 37, pp. 862-865, 2010.

[21] Y. Li and J. Li, "A highly adjustable base isolator utilizing magnetorheological elastomer: experimental testing and modeling," *Journal of vibration and acoustics,* vol. 137, Art No. 011009, 2015.

[22] J. Yang, S. Sun, T. Tian, W. Li, H. Du, G. Alici*, et al.*, "Development of a novel multi-layer MRE isolator for suppression of building vibrations under seismic events," *Mechanical Systems and Signal Processing,* vol. 70-71, pp. 811–820, 2016.

[23] Z. Xing, M. Yu, S. Sun, J. Fu, and W. Li, "A hybrid magnetorheological elastomer-fluid (MRE-F) isolation mount: development and experimental validation," *Smart Materials and Structures,* vol. 25, Art No. 015026, 2015.

[24] M. Levitt, "Spin Dynamics: Basics of Nuclear Magnetic Resonance," *Chichester: John Wiley & Sons,* 2001.